

Decarbonization potential of on-road fuels and powertrains in the European Union and the United States: a well-to-wheels assessment

Original

Decarbonization potential of on-road fuels and powertrains in the European Union and the United States: a well-to-wheels assessment / Cai, Hao; Prussi, Matteo; Ou, Longwen; Wang, Michael; Yugo, Marta; Lonza, Laura; Scarlet, Nicolae. - In: SUSTAINABLE ENERGY & FUELS. - ISSN 2398-4902. - ELETTRONICO. - 6:19(2022), pp. 4398-4417. [10.1039/D2SE00411A]

Availability:

This version is available at: 11583/2971047 since: 2022-09-07T12:19:15Z

Publisher:

Royal Society of Chemistry

Published

DOI:10.1039/D2SE00411A

Terms of use:

This article is made available under terms and conditions as specified in the corresponding bibliographic description in the repository

Publisher copyright

(Article begins on next page)

A sensor fusion strategy based on a distributed optical sensing of airframe deformation applied to actuator load estimation

Gaetano Quattrocchi
*Department of Mechanical and
Aerospace Engineering
Politecnico di Torino*
Turin, Italy
gaetano.quattrocchi@polito.it

Matteo D.L. Dalla Vedova
*Department of Mechanical and
Aerospace Engineering
Politecnico di Torino*
Turin, Italy
matteo.dallavedova@polito.it

Emanuele Frediani
*Department of Mechanical and
Aerospace Engineering
Politecnico di Torino*
Turin, Italy
emanuele.frediani@gmail.com

Paolo Maggiore
*Department of Mechanical and
Aerospace Engineering
Politecnico di Torino*
Turin, Italy
paolo.maggiore@polito.it

Pier Carlo Berri
*Department of Mechanical and
Aerospace Engineering
Politecnico di Torino*
Turin, Italy
pier.berri@polito.it

Abstract—Real-time health monitoring of mechatronic onboard systems often involves model-based approaches comparing measured (physical) signals with numerical models or statistical data. This approach often requires the accurate measurement of specific physical quantities characterizing the state of the real system, the command inputs, and the various boundary conditions that can act as sources of disturbance.

In this regard, the authors study sensor fusion techniques capable of integrating the information provided by a network of optical sensors based on Bragg gratings to reconstruct the signals acquired by one or more virtual sensors (separately or simultaneously). With an appropriate Fiber Bragg Gratings (FBGs) network, it is possible to measure directly (locally) several physical quantities (e.g. temperature, vibration, deformation, humidity, etc.), and, at the same time, use these data to estimate other effects that significantly influence the system behavior but which, for various reasons, are not directly measurable. In this case, such signals could be "virtually measured" by suitably designed and trained artificial neural networks (ANNs). The authors propose a specific sensing technology based on FBGs, combining suitable accuracy levels with minimal invasiveness, low complexity, and robustness to EM disturbances and harsh environmental conditions. The test case considered to illustrate the proposed methodology refers to a servomechanical application designed to monitor the health status in real-time of the flight control actuators using a model-based approach. Since the external aerodynamic loads acting on the system influence the operation of most of the actuators, their measurement would be helpful to accurately simulate the monitoring model's dynamic response. Therefore, the authors evaluate the proposed sensor fusion strategy effectiveness by using a distributed sensing of the airframe strain to infer the aerodynamic loads acting on the flight control actuator. Operationally speaking, a structural and an aerodynamic model are combined to generate a database used to train data-based surrogates correlating strain measurements to the corresponding actuator load.

Keywords— ANN, distributed optical sensing, Fiber Bragg Gratings, FBG, load estimation, on-board fault detection, optical fibers, prognostics, smart sensor

I. INTRODUCTION

The use of a fiber-optic based structural sensing system derives from the need to evaluate the health condition of a complex system, such as an aircraft, in a less expensive way, given the fact that aircrafts maintenance costs are one of the main expenditure items for airlines [1]. It thus follows that the use of an integrated system for structural monitoring, possibly capable of processing data in real time, is considerably advantageous in terms of overall cost reduction [2]. As briefly described in the abstract, optical fibers and thus optical sensors, such as Fiber Bragg Gratings (FBGs) possess many advantages over traditional electrical sensors, such as minimal invasiveness, low complexity, electro-magnetic disturbances insensitivity and ability to operate in harsh environmental conditions. In the framework of prognostics, the availability of accurate data (or signals) is fundamental to evaluate the current health status of a system or component, thus it is of crucial importance that the data used is as accurate and reliable as possible. These signals [3-4] can be directly representative of the current state of the monitored system or used as input signals to the surrogate model, which simulates the physical system response and allows the implementation of model-based monitoring. However, it should be noted that not all the signals required by the surrogate model are necessarily actually acquired onboard by physical sensors. Some of them, used i.e. for controlling or monitoring the system itself, will be available, but others (e.g. aerodynamic load acting on control surfaces) may be missing. In this case, rather than implementing other dedicated sensors network (with possible problems of complexity, maintenance costs, and reduced reliability), it is advisable to evaluate the possibility of obtaining the missing information using virtual sensors [5-6]. The approach presented, based on low-cost, robust, non-invasive sensors compatible with harsh environments [7], is promising and could be used in structural applications (e.g. Structural Health Management) and extended to less common areas as diagnostic or prognostic monitoring of mechatronic or electrohydraulic systems [8-10].

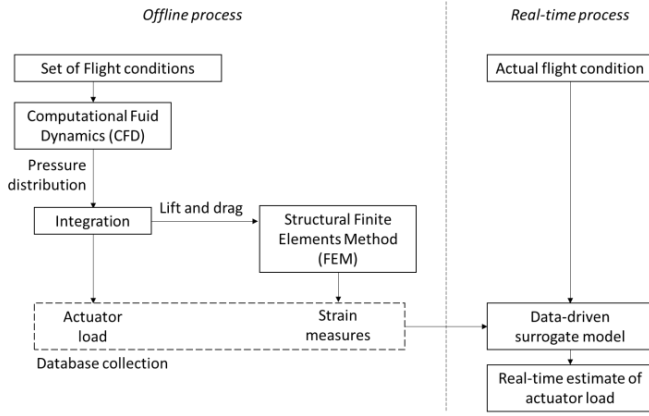


Fig. 1. Schematic of the information flow of the proposed method.

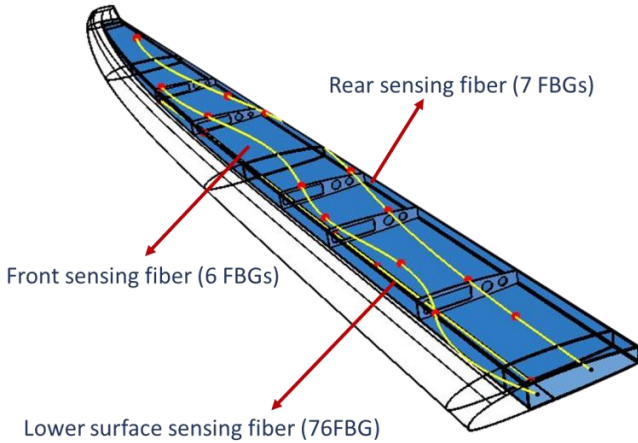


Fig. 2. Schematic configuration of the final optical sensor network.

In the particular application case of standard flight controls, actuator loads are not usually directly available as measured signals; this is due to the reliability and complexity penalties often associated with installing dedicated sensors and transducers, and thus an indirect approach based on a virtual sensor is easily favorable.

II. SCOPE OF THE WORK

The aim of this work is to present a novel method to evaluate, in real-time, the hinge moment of an aircraft aileron; the workflow is shown in Figure 1. There are two branches in this process: offline and online. This paper focuses on the offline branch, i.e. the creation of a database that will then be used in the online process as data source for a suitable data-driven surrogate model. In order to do so, a number of various different conditions has to be simulated, considering different environmental parameters but also varying deflection of the surface of interest, since the final aim of the work is to have an estimation of the hinge moment of said surface. Operatively, a battery of CFD (Computational Fluid Dynamics) and FEM (Finite Elements Method) simulation has been carried out, in order to obtain aerodynamic loads and structure deformation. In fact, the pressure field obtained for a given set of operating conditions using CFD, is used as external load for FEM analyses. The pressure distribution on the control surface is then integrated to calculate the force acting on the servoactuator.

One problem that arises is now the optimal placement of a limited number of FBG sensors on the wing, in order to maximize the accuracy of the system; in fact, FBGs sense the deformation only at a particular spatial point [11] - this concept has been already explored in [12]; all of these measurements will then be used as input for an ANN (Artificial Neural Network), including other relevant data such as atmospheric data and attitude information obtained by other on-board instruments. In this sense, this is a sensor-fusion approach. After training, the ANN output will be the hinge moment using present-time flight conditions. Given the complexity of the method, in this paper only the first part of the process will be explored, i.e. databases generation and sensors optimal placement.

III. MODEL DEFINITION

The aircraft used in this work is an electric, solar-powered UAV (Unmanned Aerial Vehicle), RA, conceptualized and designed (Fig. 3) by students team Icarus at Politecnico di Torino. The vehicle adopts a conventional high wing configuration, with a 5 m wingspan. Fuselage is bubble shaped, with a length of 2 m; the tail is T-shaped, with 0.5 m height. Propulsion is achieved using a single 50 cm propeller placed in the front of the fuselage, actuated by one electric motor. External surfaces and main structural components are made using composite materials. In Fig. 4 a CAD model of the wing is shown. The battery pack (red), that is used for storing energy, is placed inside the wing in order to maximize the moment of inertia on the roll axis of the aircraft, thus improving controllability. In the main structure, three main elements are visible:

- Skin (light blue), made of laminated carbon fiber (two $\pm 45^\circ$ layers), holding the aerodynamic shape of the wing;
- Wingbox (yellow), made of laminated carbon fiber (two $\pm 90^\circ$ layers), that is the main structural element;
- Ribs (gray), made of sandwich composite, with the faces made of three layers of laminated carbon fiber and Rohacell core, used for longitudinal strengthening and skin shaping.

Further dimensional details are visible in Fig. 5.

IV. FLIGHT CONDITIONS

As previously said, a database of different combinations of flight conditions and command inputs has to be generated. To limit the number of simulations to a reasonable level, the assumption of constant temperature, pressure and density is made, considering ISA standard atmospheric conditions, i.e. $p = 1.01 \cdot 10^5$ Pa, $T = 15$ °C, at zero altitude, i.e. density $\rho = 1.225$ kg/m³. The variables that have been varied to obtain different combinations are speed V , angle of attack α and surface deflection δ_a . In particular, values around nominal flight conditions ($V = 15$ m/s, $\alpha = 3.5^\circ$) will be considered. In total, the number of combinations selected is 41, that are distributed in the following way (expressed in condensed form):

- (1) $V = 15$ m/s
 - (a) $\alpha = 2^\circ$: $\delta_a = [0, \pm 5, \pm 10, \pm 15, \pm 20]^\circ$;
 - (b) $\alpha = [5, 8]^\circ$: $\delta_a = [0, \pm 5, \pm 10, \pm 15]^\circ$;
- (2) $V = [5, 10]$ m/s
 - (a) $\alpha = [2, 5, 8]^\circ$: $\delta_a = [0, \pm 5]^\circ$;

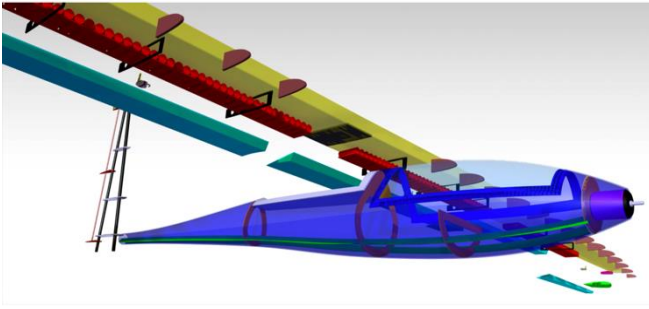


Fig. 3. Overall view of the model aircraft.

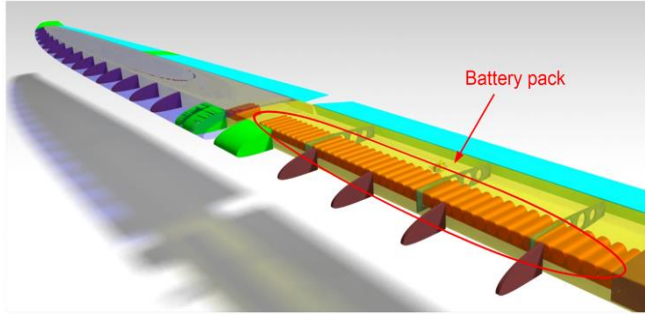


Fig. 4. Aircraft wing view.

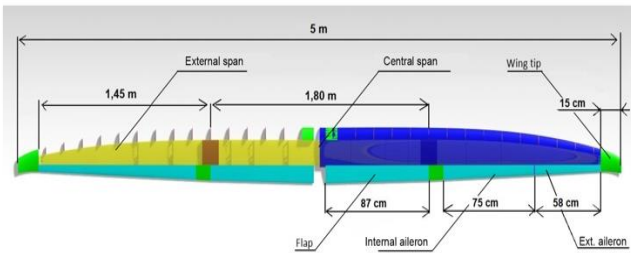


Fig. 5. Geometrical detail of the wing.

V. CFD ANALYSIS

After the creation of a suitable number of test conditions, the following step is to evaluate the stress condition on the wing deriving from the particular operation point. In order to do so, CFD analysis will be carried out firstly to evaluate the pressure field on the wing and thus the distributed load acting on it. Furthermore, the integration of the pressure field on the aileron surface gives an estimation of the load acting on the servoactuator shaft. The software used for CFD simulations is Star-CCM+.

A. Simulations details

Given the symmetrical nature of the problem along the longitudinal axis, the computational domain has been chosen as an hemisphere rather than simulating the whole spherical domain. The radius of the domain is $R_d = 20$ m, which is 8x the wing span. The elements chosen are polyhedral cells, which have more interfaces compared to traditional cells. In presence of a complex flow field, such as the one generated in proximity of a wing, polyhedral cells show better residual at convergence and generally require less iterations. Cell size is variable, as visible in Fig.6, with smaller size in proximity of the profile itself; furthermore an inflation layer is present on the profile itself, composed by 25 prism cell stacked normally to the boundary. The scope of these layers is to better capture the boundary layer.

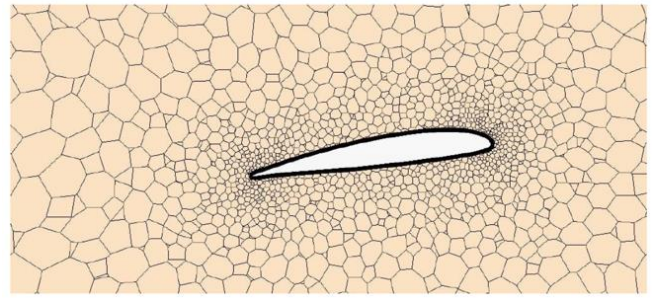


Fig. 6. Mesh view in proximity of the wing.

Regarding boundary conditions, a free stream condition is imposed along the external boundary of the computation domain, while a symmetry condition is imposed on the longitudinal plane; finally, a wall condition is imposed on all vehicle surfaces in contact with the airflow. The fluid modeling adopted is a RANS (Reynolds Averaged Navier Stokes) solution model, since the detailed temporal evolution of the flow is not of interest (i.e. steady-state solution is of importance). For turbulence, an approach called SST $k - \omega$ with $\gamma - Re\theta$ transition is adopted, which is a hybrid method that mixes two different turbulence models using different weights depending on wall distance [13].

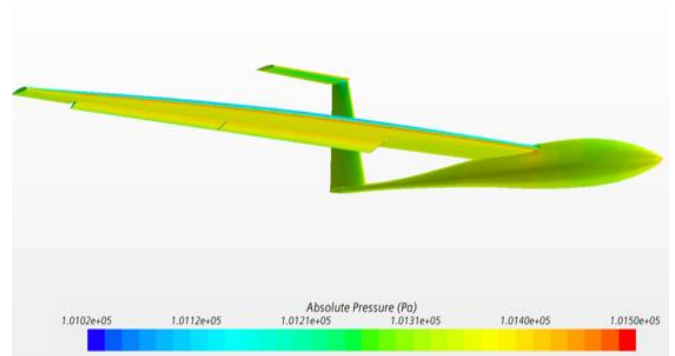


Fig. 7. Pressure field for cruising conditions ($V = 15$ m/s, $\alpha = 2^\circ$).

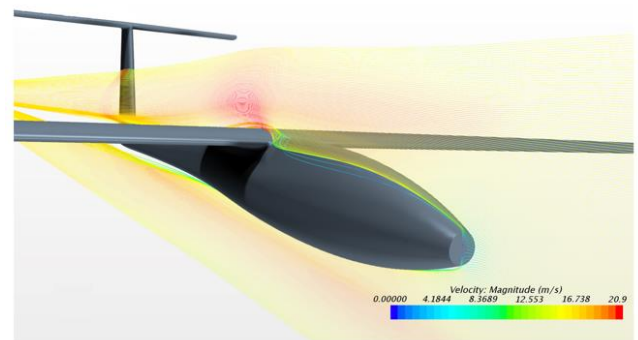


Fig. 8. Longitudinal plane velocity field for cruising conditions ($V = 15$ m/s, $\alpha = 2^\circ$).

VI. FEM ANALYSIS

After having simulated the external flow field in order to evaluate the pressure distribution along the wingspan, it is now possible to simulate the wing deflection using FEM. The model has been suitably simplified from its original detail level in order to maintain only the most significant features.

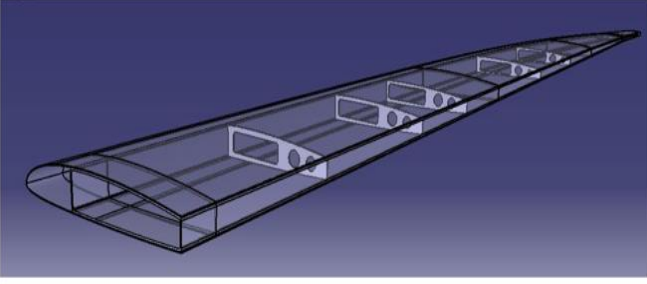


Fig. 9. CAD view of the simplified wing model used for FEM analysis.

All the simulations have been carried out using the Altair Hyperworks suite; Hypermesh has been used for meshing, material assignment and external load definition. Optistruct is the numerical solver itself and Hyperview has been used to create the post-processed plots.

A. Simulations details

Since the region of interest is the wing structure, the FEM simulations will only consider the wing, modeling the wing-fuselage insertion as a rigid connection, i.e. imposing zero- displacement conditions for all degrees of freedom for all nodes laying on the symmetry plane. Regarding loads, two types of loads are applied: inertial and aerodynamic. Inertial loads are automatically evaluated by the solver and accordingly applied to the elements affected; the battery pack is not structural mass and thus has to be manually added, as distributed loads, for the computation. The two battery packs have linear mass of 2.5 kg/m for the internal one (800 mm length, 40 batteries) and 1.625 kg/m for the external one (650 mm length, 32 batteries). Aerodynamic loads have been evaluated in the previous step using CFD, and thus are simply transferred on the wing surfaces mesh using the *field* function, mapping the relevant values of pressure to each relative element. Furthermore, the concentrated loads acting on the shafts of the servoactuators have been calculated and applied; the calculation is based on an integration of the pressure differential across the aileron surface and thus obtaining the hinge moment and the two forces acting on the actuator rod (along the x and y directions).

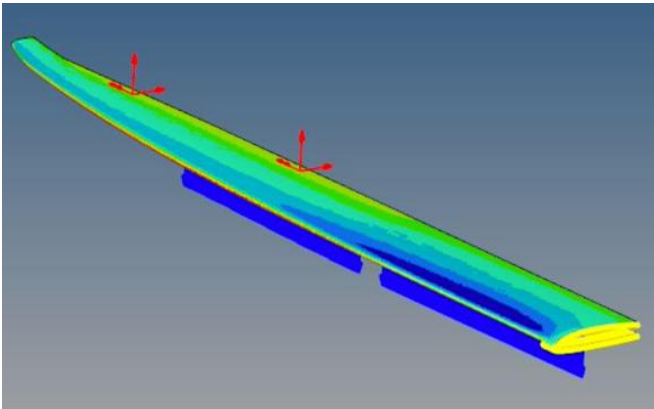


Fig. 10. Loads applied for the FEM simulations: the dark blue arrows represent the inertial load of the battery packs; the red arrows are the concentrated forces acting on the servoactuators rods; the blue-green shading is the pressure field. Finally, on the root chord, the yellow elements are all the nodes with zero-displacement constraint.

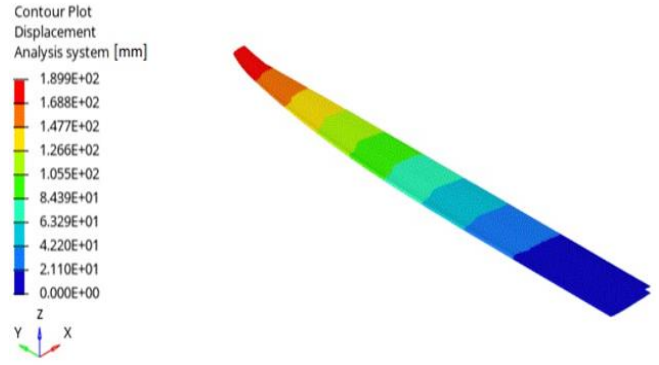


Fig. 11. Wing displacement during cruise conditions.

All the wing structures are made from carbon fiber reinforced plastics (CFRP), with different properties depending on the function they have. The carbon fabric used for all elements is TeXtreme Carbon Fabric 80 g/m², with the following mechanical properties: $E = 240$ GPa, $\sigma_{\text{break}} = 4.8$ GPa, $\rho = 1.79$ g/cm³, $d = 7$ μm , where d is the fibers diameter. The resin used in the composites is the SX10 epoxy, mixed with a 40% resin to 60% fiber proportion. The mechanical properties for a single layer, calculated using the Multiscale Designer tool, are $E_x = 85$ GPa, $E_y = 85$ GPa, $G_{xy} = 11.56$ GPa, $\nu_{xy} = 4.27 \cdot 10^{-3}$, $\rho = 1.55 \cdot 10^{-3}$ g/mm³, where E is the elasticity modulus, G is the shear modulus, ν is the Poisson ratio and ρ is the density. As previously stated, each element is engineered as to maximize the required performance while minimizing the mass, and this is achieved by optimal layering of the composite layers. The following scheme describes the lamination scheme for the components:

- Skin: two layers at $\pm 45^\circ$;
- Wingbox: two layers at $\pm 90^\circ$;
- Ribs: eight layers, four at $+45^\circ$ and four at -45° .

VII. RESULTS AND CONCLUSIONS

After carrying out all the simulations, the data are logged in a single .csv file. All the relevant information obtained (stresses, strains, displacements) will be then used, using a proper algorithm, to evaluate the optimal FBGs placement strategy as to have the best sensitivity to strain conditions while minimizing the number of sensors used. In Fig. 11 the displacement of the wing in cruise flight is depicted. As expected, there are discrete variation of the displacement value after each rib, with the highest displacement at the wingtip. As described in the introduction, this work is only a small part needed to create a complex prognostics and diagnostic framework (Fig. 1). This work had the task of creating a dataset of external conditions and relative stress/displacement statuses of the wing structure, whose scope will be to train a neural network or suitable alternative machine learning method in order to predict the aileron hinge moment given a particular set of external condition (velocity, angle of attack) and command (aileron deflection angle).

In order to do so, the next step will be to evaluate the best possible locations for placing a moderate number of FBGs sensors along the wing, in order to have punctual evaluation of the strain field and thus, using interpolation, an approximation of the wing global strain field.

REFERENCES

- [1] M. J. Dupuy, D. E. Wesely, and C. S. Jenkins, "Airline fleet maintenance: Trade-off analysis of alternate aircraft maintenance approaches," 2011 IEEE Systems and Information Engineering Design Symposium, pp. 29–34, 2011.
- [2] T. Dong, and N. H. Kim, "Cost-effectiveness of structural health monitoring in fuselage maintenance of the civil aviation industry," *Aerospace*, vol. 5, n. 3, paper 87, 2018.
- [3] C. Byington, W. Watson, D. Edwards, and P. Stoelting, "A Model-Based Approach to Prognostics and Health Management for Flight Control Actuators," IEEE Aerospace Conf. Proceedings, 2004.
- [4] F. Vachtsevanos, F. Lewis, M. Roemer, A. Hess, and B. Wu, *Intelligent Fault Diagnosis and Prognosis for Engineering Systems*, Wiley, 2006.
- [5] P. C. Berri, M. D. L. Dalla Vedova, and L. Mainini, "Learning for prediction: real-time reliability assessment of aerospace systems," 2021 AIAA SciTech Forum (AIAA 2021-1478), 2021.
- [6] P. C. Berri, M. D. L. Dalla Vedova, A. Laudani, P. Maggiore and C. Secci, "Study of packaging and installation of FBG sensors for monitoring of aircraft systems," Proc. of the 30th European Safety and Reliability Conf. and the 15th Probabilistic Safety Assessment and Management Conf., pp. 3599-3606, 2020.
- [7] J. Santos and F. Farahi, *Handbook of Optical Sensors*, CRC, 2018.
- [8] P. C. Berri, M. D. L. Dalla Vedova, and P. Maggiore, "A Smart Electromechanical Actuator Monitor for New Model-Based Prognostic Algorithms," *International Journal of Mechanics and Control*, vol. 17, n. 2, pp. 19–25, 2016.
- [9] P. C. Berri, M. D. L. Dalla Vedova, and P. Maggiore, "On-board electromechanical servomechanisms affected by progressive faults: proposal of a smart GA model-based prognostic approach," Proc. of the 27th European Safety and Reliability Conference (ESREL 2017), pp. 839–845, Portoroz, Slovenia, June 18-22, 2017.
- [10] M. Battipede, M. D. L. Dalla Vedova, P. Maggiore, and S. Romeo, "Model based analysis of precursors of electromechanical servomechanisms failures using an artificial neural network," Proc. of the AIAA SciTech Modeling and Simulation Technologies Conference, 2015. <http://dx.doi.org/10.2514/6.2015-2035>
- [11] Z. Ma, and X. Chen, "Fiber Bragg Gratings sensors for aircraft wing shape measurement: Recent applications and technical analysis," *Sensors*, vol. 19, n. 1, paper 55, 2019.
- [12] P. C. Berri, C. Corsi, M. D. Dalla Vedova, A. D. Laudani, P. Maggiore, and C. Secci, "Study of packaging and installation of FBG sensors for monitoring of aircraft systems," Proceedings of the 30th European Safety and Reliability Conference and the 15th Probabilistic Safety Assessment and Management Conference, Research Publishing, 2020.
- [13] H. Shah, S. Mathew, and C. M. Lim, "Numerical simulation of flow over an airfoil for small wind turbines using the $\gamma - Re_{\theta}$ model," *International Journal of Energy and Environmental Engineering*, vol. 6, n. 4, pp. 419–429, 2015.